Received: 1 April 2020 | Revised: 14 August 2020 | Accepted: 15 August 2020

DOI: 10.1002/jssc.202000372

JOURNAL OF SEPARATION SCIENCE

RESEARCH ARTICLE

Investigation of the enantioselective interaction between selected drug enantiomers and human serum albumin by mobility shift-affinity capillary electrophoresis

Ratih Ratih[1,2] | **Hermann Wätzig**[1] | **Matthias Stein**[1] | **Sami El Deeb**[1]

[1] Institute of Medicinal and Pharmaceutical Chemistry, Technische Universität Braunschweig, Braunschweig, Germany

[2] Department of Pharmaceutical Chemistry, Faculty of Pharmacy, University of Surabaya, Surabaya, Indonesia

Correspondence
Prof. Sami El Deeb, Institute of Medicinal and Pharmaceutical Chemistry, Technische Universität Braunschweig, Beethovenstr. 55, 38106 Braunschweig, Germany.
Email: s.eldeeb@tu-braunschweig.de

Funding information
Indonesia Endowment Fund for Education (LPDP), Ministry of Research, Technology and Higher Education (RISTEK DIKTI), Republic of Indonesia

Mobility shift-affinity capillary electrophoresis was employed for enantioseparation and simultaneous binding constant determination. Human serum albumin was used as a chiral selector in the background electrolyte composed of 20 mM phosphate buffer, pH 7.4. The applied setup supports a high mobility shift since albumin and the drug-albumin complex hold negative net charges, while model compounds of amlodipine and verapamil are positively charged. In order to have an accurate effective mobility determination, the Haarhoff-van der Linde function was utilized. Subsequently, the association constant was determined by nonlinear regression analysis of the dependence of effective mobilities on the total protein concentration. Differences in the apparent binding status between the enantiomers lead to mobility shifts of different extends (α). This resulted in enantioresolutions of *R*s = 1.05–3.63 for both drug models. *R*-(+)-Verapamil (K_A 1844 M^{-1}) proved to bind stronger to human serum albumin compared to *S*-(−)-verapamil (K_A 6.6 M^{-1}). The association constant of *S*-(−)-amlodipine (K_A 25 073 M^{-1}) was found to be slightly higher compared to its antipode (K_A 22 620 M^{-1}) when applying the racemic mixture. The low measurement uncertainty of this approach was demonstrated by the close agreement of the association constant of the enantiopure *S*-(−)-form (K_A 25 101 M^{-1}).

KEYWORDS
affinity capillary electrophoresis, amlodipine, enantioselective interaction, human serum albumin, mobility-shift assay

1 | INTRODUCTION

The stereoselectivity of a living body exhibits different affinities toward a pair of enantiomers, which results in diverse pharmacology, pharmacokinetics, metabolism, and toxicology [1]. The binding affinity represents the strength of the binding interaction between a molecule and a binding site [2]. Information on a feasible interaction

Article Related Abbreviations: AML, amlodipine; CCB, calcium-channel blocker; CS, chiral selector; FA, frontal analysis; HVL, Haarhoff-van der Linde; LPC-CE, liquid pre-column capillary electrophoresis; ms-ACE, mobility shift-affinity capillary electrophoresis; VER, verapamil

is valuable in chiral analysis, particularly in developing enantioseparation methods and predicting drug behavior in the biological system [3]. Thus, drug quality control and treatment for patients can be optimized by understanding the molecular interactions.

Molecular interactions in the biological system are mostly related to the availability of human serum proteins. HSA and α-acid glycoprotein are the most important transporter proteins due to their ability to bind to a wide variety of drugs [4–6]. HSA is a single-chain, nonglycosylated polypeptide containing 585 amino acid residues with a molecular mass of 66.5 kDa. In the circulatory system, HSA represents about 60% of the total plasma proteins at typical concentrations of 30–50 g/L [7]. It plays an important role as a carrier of endogenous ligands and intrinsically exhibits high stereoselectivity [4]. Due to its stereoselectivity in binding, HSA is an ideal candidate for studying protein–enantiomer interactions of the human body.

Since calcium-channel blockers (CCBs) are produced and marketed as racemic mixtures, it is important to investigate the binding affinity of the individual enantiomers. A clinical study on CCBs has reported high protein binding for amlodipine (AML) and verapamil (VER) with different duration of actions. Protein binding and elimination half-life ($t_{1/2}$) of AML were found to be more than 99%; $t_{1/2}$ 42.5 h and VER 84–93%; $t_{1/2}$ 3.2 h [8]. Consider the difference between AML and VER in pharmacokinetic profiles: both racemic mixtures were selected as chiral drug models to study the stereoselectivity interactions toward HSA.

AML is a dihydropyridine CCB used as a treatment choice of hypertension and coronary artery disease [9,10]. The chemical structure of AML possesses an asymmetric carbon atom, resulting in the existence of *R*-(+)- and *S*-(−)-enantiomers. It has been marketed as a racemate, known as amlodipine benzene sulfonic acid salt (besylate). However, both enantiomers do not possess the same potency as calcium channel inhibitors. The *S*-(−)-enantiomer of AML shows the antihypertensive effect, which is approximately 1000 times stronger than the *R*-(+)-enantiomer [10]. Therefore, the *S*-(−)-form is considered to be most responsible as CCB-mediated pharmacodynamics action [11]. These facts clearly show that the stereochemistry of AML plays an important role in the enantiomeric composition of pharmaceuticals and its pharmacological effects. Another treatment choice for hypertension and coronary artery disease is VER, a phenylalkylamine [9]. VER has one chiral center, and thus two enantiomers of *R*-(+)-VER and *S*-(−)-VER exist. The pharmacological activity of *S*-(−)-VER is found to be 10–20 times more potent compared to its antipode. Even though it is less potent in calcium channel inhibition, *R*-(+)-VER showed potential anti-tumor activity [12].

HSA–drug interaction studies of AML and VER have been conducted by several analytical methods such as spectroscopy, chromatography, and CE. Fluorescence and circular dichroism spectroscopy have been developed for AML binding constant determination [13] and frontal analysis (FA) high-performance affinity chromatography for association equilibrium constant assay of VER enantiomers [14]. Moreover, various CE-based analytical methods to assess the binding affinity parameters of chiral drugs toward HSA have been developed [15–17]. Liu et al. have investigated the interaction of AML enantiomers to HSA by flow injection-CE frontal analysis (FI-CE/FA) [18]. A CE/FA method has been employed for molecular association study of VER enantiomers in a racemic mixture toward HSA [19]. Chiral CE offers possibilities to immobilize the selector onto a silica capillary surface [20,21] as well as to operate in a free solution that does not require the immobilization of the chiral selector (CS). In general, a basic prerequisite of enantiomeric separations in CE is that at least one of the counterparts is charged. The separation requires a sufficient stereoselective interaction between enantiomers and the CS. Combination methods of CE/FA for measuring unbound enantiomers together with trimethyl-β-cyclodextrin based enantioseparation in free solution was employed in the binding constant determination of *R*-(+)-VER and *S*-(−)-VER [22]. The reported K_A values of both VER enantiomers have closely agreed with a previous study using liquid pre-column CE [23]. Although these CE methods were intended to study stereoselective interactions of HSA-drug enantiomers, none of them performed the enantioseparation using HSA as a CS. Since a racemic mixture contains two enantiomers, a method for HSA-based enantioseparation and simultaneous binding constant determination is challenging to develop.

Among the established methods of binding studies [24], ACE is well suited to enantiomeric separations [25] and simultaneous binding constant determination [26,27]. ACE offers various separation modes in the field of enantioselective investigation [24,27]. Combinations of CE with equilibrium dialysis and CE with ultrafiltration have been used for binding evaluation of AML [28] and fluoxetine [29], respectively. Different modes of ACE using HSA as a selector have been developed for assessing noncovalent binding [27]. HSA can hold positively or negatively net charges, depending on the pH value of the BGE. The common approaches rely on measuring alternations of size, shape, or charge due to the complexation [24,25,27]. In terms of the protein additive in the BGE for a direct separation, ACE is also known as mobility shift-affinity CE (ms-ACE) [30,31]. A baseline enantiomeric separation of omeprazole using HSA as a CS was achieved by ms-ACE mode [26].

The main purpose of chiral separation methods is to generate a baseline enantioseparation. Along with it, the affinity constant represents the strength of the interaction between individual enantiomers with the CS or the distinction migration of the two enantiomer–CS complexes [32]. Determining the binding constant is not only valuable in assessing the strength of the complex reaction but can also be applied to optimize the chiral separation, for example, selection of a suitable concentration of the CS [33,34]. The estimation of binding constants offers an efficient step of structured analytical research for an enantioselective interaction study in the method development, which is challenging.

This study was carried out to evaluate enantioselective interaction between selected drug enantiomers and HSA, including enantiomeric separation and simultaneous binding constant determination by ms-ACE. In order to have an accurate mobility determination, the Haarhoff-van der Linde function was utilized [35]. Electrophoretic parameters of resolution and effective mobility were evaluated. Subsequently, association constants were determined through nonlinear regression of effective mobilities as a function of total ligand concentration.

2 | MATERIALS AND METHODS

2.1 | Reagents and solutions

Human serum albumin (lyophilized powder ≥ 97%), disodium hydrogen phosphate (Na_2HPO_4), sodium hydroxide (NaOH), sodium dodecyl sulfate (SDS) ≥ 98.5%, phosphoric acid (H_3PO_4) 85%, acetone (CH_3COCH_3) ≥ 99.9%, (*R*, *S*)-amlodipine (as amlodipine besylate), and (*R*, *S*)-verapamil were acquired from Sigma-Aldrich Chemie (Steinheim, Germany). The *S*-(−)-amlodipine was obtained from Biozol Diagnostica Vertrieb (Munich, Germany). The water was purified by Arium® pro UF/VF-Sartophore 0.2 μm water purification system from Sartorius Weighing Technology (Gottingen, Germany).

The phosphate buffer was prepared using 20 mM disodium hydrogen phosphate and adjusted by phosphoric acid 85% (≈0.4 mL) to reach the final pH 7.4 of 1 L buffer solution. Solutions of 30 mM SDS, 1 M NaOH, and 0.1 M NaOH were prepared in ultrapure water. All the solutions were filtered using nylon membrane 0.22 μM pore size from Rotilabo®-syringe filter (Karlsruhe, Germany) prior to the analysis.

A series of background electrolyte was prepared by spiking HSA at various concentrations of 30–110 μM into 20 mM phosphate buffer solution pH 7.4. Stock solutions of (*R*, *S*)-AML and *S*-(−)-AML were predissolved in 10% v/v methanol at 1.0 mg/mL. A fixed aliquot of 300.0 μg/mL of both stock solutions was diluted with 20 mM phosphate buffer pH 7.4. The stock solution of (*R*, *S*)-VER was prepared in 60% v/v methanol at 1.0 mg/mL and subsequently dissolved in 20 mM phosphate buffer pH 7.4 to the final concentration of 600.0 μg/mL. The working solution of each drug was prepared by spiking 2% v/v acetone into a certain volume of the diluted stock solution. Samples containing the individual drugs were injected six times ($n = 6$) for each BGE condition.

2.2 | Instrumentation

The chiral study has been performed with a PrinCE CEC-760 system (Prince Technologies, Emmen, the Netherlands) using a diode array UV-Vis detector (190–600 nm). The DAx 3D software was used for instrumental control, data acquisition, and data analysis. Bare fused-silica capillary from Polymicro Technologies (Phoenix, AZ, USA) with a dimension of 50 μm inner and 360 μm outer diameters, 53.5 cm total length, and 45 cm effective length was used throughout the study. The sample rack and capillary oven were set at 25°C.

2.3 | Software

Data were evaluated using Microsoft excel 2010 (Microsoft, Redmont, WA, USA). The K_A and μ_c values were calculated using Origin 2018 64 Bit (©OriginLab Corporation, Northampton, MA, USA) and CEVal [35] (Capillary Electrophoresis Evaluator at https://enchmet.natur.cuni.cz/software/ceval), respectively.

2.4 | Mobility shift-affinity CE procedure

In the general scheme of ms-ACE, the entire capillary and the running BGE vials are filled with BGE containing the CS at various concentrations from zero to a certain level. The other binding partner is injected as a small sample plug in the capillary. Subsequently, when high voltage is applied, the enantiomers will be separated according to their individual effective electrophoretic mobilities. Due to different degrees of complexation, the enantiomeric analytes will hold different apparent mobilities depending on the CS levels [32,36]. The change of effective mobilities as a function of the ligand concentrations is used to calculate the apparent binding properties in ms-ACE [37]. A schematic illustration of the ms-ACE setup is given in Figure 1.

The new capillary was pretreated using 1 M NaOH (30 min), 0.1 M NaOH (10 min) and ultrapure water

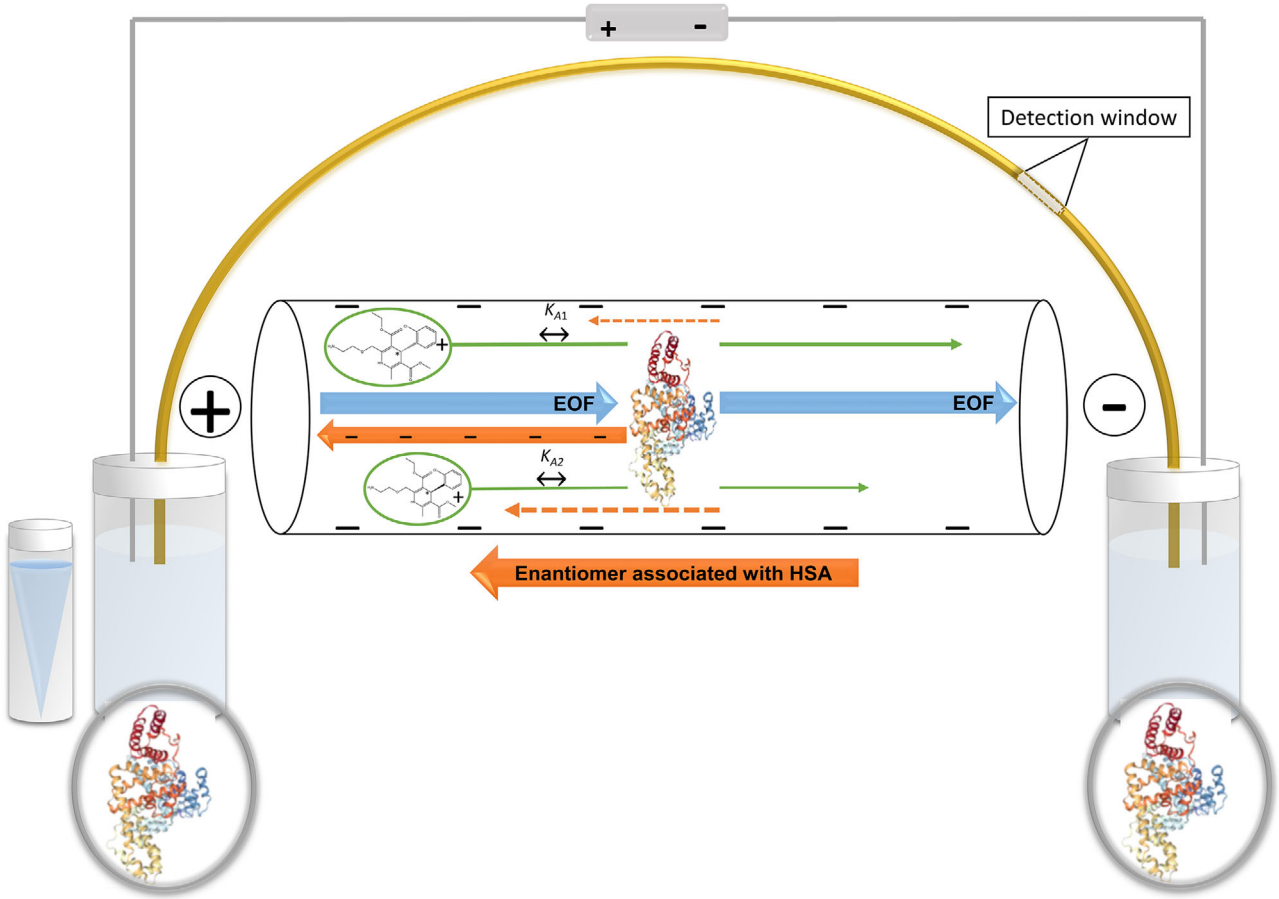

FIGURE 1 Schematic illustration of enantioselectivity in the applied ms-ACE system

(10 min). At the beginning and the end of the analysis, the capillary was flushed using 0.1 M NaOH and followed by ultrapure water for 10 min. All rinsing steps were performed using 1500 mbar pressure. An interval rinsing between each injection was applied using 30 mM SDS (1500 mbar, 1 min), ultrapure water (1500 mbar, 0.5 min), 0.1 M NaOH (1500 mbar, 1 min), ultrapure water (1500 mbar, 0.5 min), and BGE (1500 mbar, 2 min). Finally, samples were injected into the capillary for 6 s with a pressure of 50 mbar. All separations were conducted at 25°C using 15 kV applied voltage with the cathode at the capillary outlet.

The enantioselective interactions were investigated using HSA at concentrations of 0, 30, 40, 50, 70, 90, and 110 μM. The pure BGE contains 20 mM disodium hydrogen phosphate at pH 7.4. Selected drugs of AML and VER were traced by UV detection at λ 250 nm and 240 nm. Even though HSA interferes with detection sensitivity at the selected UV wavelengths, the earlier studies by Tanaka et al. and Haginaka et al. reported the repeatabilities of migration times and peak areas were insignificantly affected [30,38]. Moreover, the measurement in ms-ACE was based on the determination of the effective mobility by evaluating the a_1 parameter of the Haarhoff–van der Linde function, which is robust toward background absorption [35]. This approach could minimize the detection sensitivity issue, thus having less effect on the applied full-filling technique of the ms-ACE system. In order to avoid ligand and/or buffer depletion of the separation system, the position of both ends (inlet and outlet) capillary were immersed into the BGE vials, alternatively.

2.4.1 | Enantiomeric resolution

The resolution (*R*s) values of two enantiomers were calculated based on the difference in the migration times and the width of the peaks at the half-height by DAx 3D software, according to the following equation:

$$Rs = 1.177 \times \frac{(t_2 - t_1)}{(W_{hh_1} + W_{hh_2})} \quad (1)$$

where t_1 and t_2 are the migration times of the individual enantiomers 1 and 2, correspondingly. Similarly, W_{hh_1} and W_{hh_2} are the widths at the half-height of peaks 1 and 2, respectively [39,40].

2.4.2 | Association constant determination

Specific chemical responses of the ms-ACE system are determined as surrogates since the degree of binding is not directly measurable [41]. The association constant (K_A) is obtained by nonlinear regression analysis via fitting the analyte's effective mobility (dependent variable, μ_i) to the corresponding selector concentration (independent variable, C_i). The model function is described by Equation (2), where μ_f is the effective mobility of the analyte in the BGE free of the selector (HSA) and μ_c is the ionic mobility of the analyte–selector complex.

$$\mu_i = \mu_f + \frac{(\mu_c - \mu_f) \times K_A \times C_i}{1 + (K_A \times C_i)} \left[\mathrm{m^2\ V^{-1}\ s^{-1}}\right] \quad (2)$$

3 | RESULTS AND DISCUSSION

3.1 | Enantiomeric separation

Due to its simplicity, a direct separation approach by adding a CS into the BGE solution is the most commonly utilized in chiral CE [29, 40, 42]. The employed CS can be easily adjusted to the optimal concentration [42,43]. Hence, having an isoelectric point of 4.7 makes HSA a negatively charged molecule at the applied physiological pH 7.4, while basic drugs such as AML (pK_a 8.6) and VER (pK_a 8.9) are positively charged. Thus, all molecules will have electrophoretic mobilities. Therefore, the enantiomers of both drugs were electrophoretically separable in the presence of HSA at the selected physiological pH [43].

An initial resolution of enantiomers with *R*s = 1.1 (AML) and *R*s = 1.0 (VER) was obtained in the addition of 30 μM HSA. The increment of HSA up to 40 μM steadily led to a partial separation, while at a 50 μM, an improvement in baseline separation was achieved. Likewise, starting at 70 μM HSA, the resolution of AML raised dramatically, whereas VER increased gradually. From the molecular point of view, noncovalent binding results in the formation of diastereomeric complexes. An increase in the concentration of HSA results in a higher α, and thus, in an overall reduction of cathodic migration [42]. Throughout the elongation of the migration times, HSA has a strong interaction with enantiomers and contributes to the enhancement of enantioresolution [16].

An interesting separation phenomenon emerged at 70 μM HSA when the effective mobility of *S*-(−)-AML switched to be more negatively charged and appeared after the EOF marker (Figure 2A). The presence of HSA significantly influenced the *S*-(−)-AML enantiomer, resulting in higher mobility and consequently possessing longer migration time. It shows that the migration of enantiomers depends on the mobility effects in the applied separation system [44].

Further increase in HSA concentration led to peak broadening, as seen in Figure 2 at 90 μM HSA. In some cases of using protein-based CS, this occurrence is likely due to protein adsorption onto the wall of the unmodified fused-silica capillaries. The extent of adsorption might increase in the presence of more amino groups and an overall more positive charge on proteins. In this study, sufficient rinsing between runs using SDS was applied to remove the adsorbed HSA and ensure the repeatability [26,30]. SDS has shown effectiveness in washing a capillary wall by the combination of denaturation proteins and micellar effect [26]. Accordingly, HSA adsorption onto the capillary wall was minimized, which prevented the separation system from severe peak broadening. Indeed, the repeatability of *Rs* values and migration times was less than 3% RSD in the range of 30–110 μM HSA as a CS. Due to the enantiomers interacting more strongly with the CS at higher concentrations [16,45], the effect of slow binding equilibrium kinetics gets more pronounced [45]. This assumption was far reasonable behind the peak broadening [45]. Strong protein–drug interaction as a result of slow kinetics binding equilibrium was shown by AML enantiomers with its broad peaks. In addition, Zhu et al. reported that the concentration of HSA dissolved in the running buffer mainly controls the efficiency of enantioseparation rather than the HSA adsorbed to the capillary wall [16]. For these reasons, the reliable enantioseparation was conducted in an optimum HSA content in the BGE from 30 to 110 μM.

Overall, within the concentration range of 30–110 μM HSA, AML showed excellent resolution with broad peaks width, while VER displayed satisfactory resolution and sharp peaks. Repeatabilities of the migration times and the *R*s values were found to be less than 1.85% RSD and 3.80% RSD for all tested analytes. HSA concentration of 50 μM was considered to be optimal as CS for AML and VER enantioseparations with a resolution of *Rs* = 1.68 and *Rs* = 1.56, respectively. The difference in binding status between enantiomers initiates the resolution, which carries out the migration of *R*-(+)-AML and *S*-(−)-VER as the first eluted peak. *S*-(−)-AML and *R*-(+)-VER possess a higher binding affinity toward HSA, compared to their antipodes. The enantioseparation profiles of AML and VER are shown in Figure 2A and B, respectively.

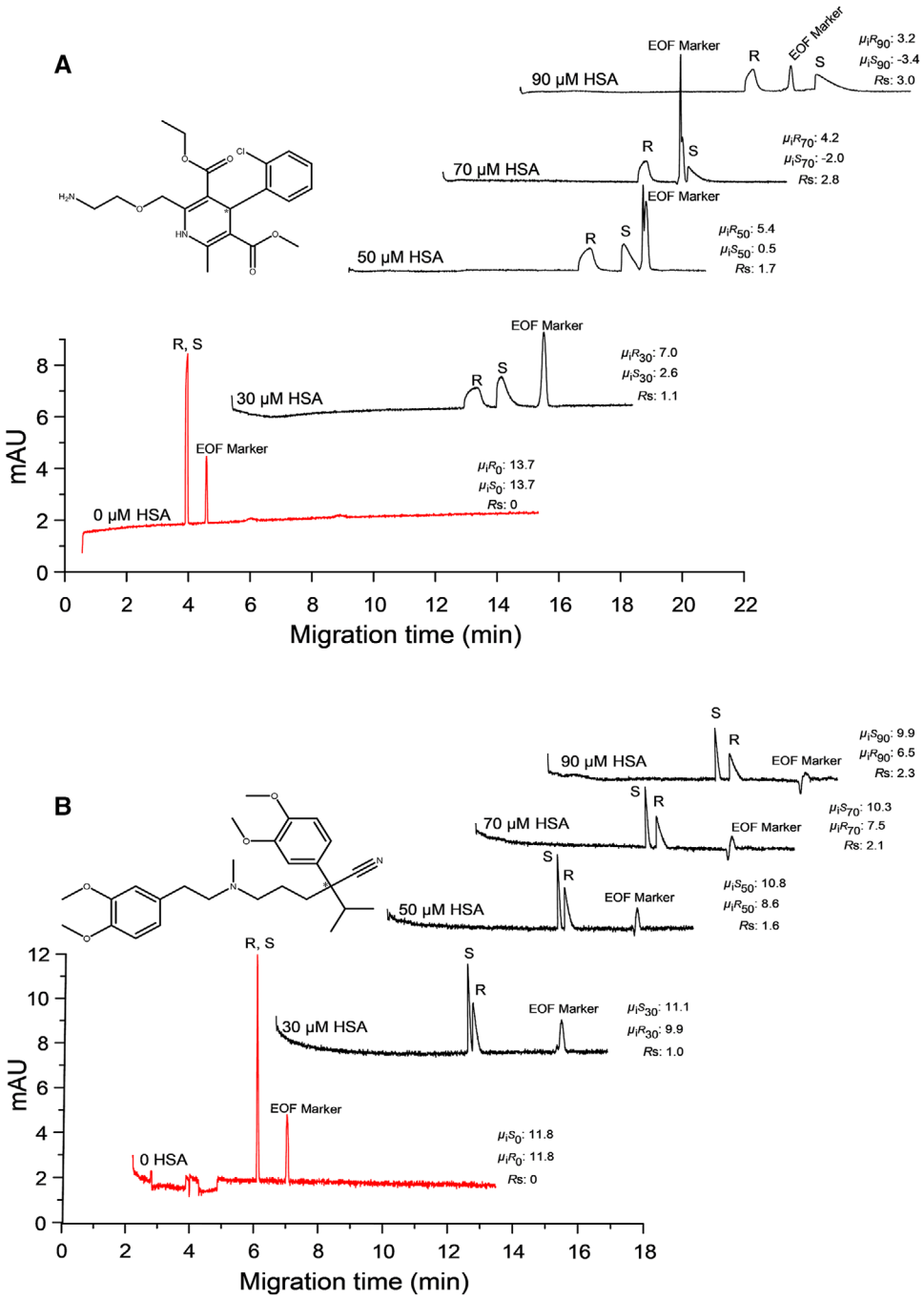

FIGURE 2 Effect of HSA concentrations on the degree of interactions toward amlodipine (AML, 2A) and verapamil (VER, 2B), which results in enantioresolutions and mobility shifts. The electropherograms show five of seven enantioseparations at the applied ms-ACE conditions, as described in the experimental section

3.2 | Binding constant determination

Further investigation of enantioselective interactions between HSA and drug models was achieved by ms-ACE using a pH and buffer composition close to the physiologically relevant conditions. Mobility shifts of the individual enantiomers as a function of HSA concentrations were evaluated simultaneously. The effective mobility of AML and VER in the absence of HSA was found to be 13.7×10^{-9} and 11.8×10^{-9} $m^2\ V^{-1}\ s^{-1}$, respectively. In the presence of 30–110 μM HSA, the first eluting enantiomer of AML and VER shifted its effective mobility from 7.00×10^{-9} to 2.20×10^{-9} and from 11.1×10^{-9} to 9.2×10^{-9} $m^2\ V^{-1}\ s^{-1}$, respectively.

TABLE 1 Effect of HSA concentrations on the enantioseparation parameters of amlodipine (AML) and verapamil (VER)

HSA	AML				VER			
[10(6 M]	μ_{i_R}	μ_{i_S}	$\Delta\mu_i$	*Rs*	μ_{i_S}	μ_{i_R}	$\Delta\mu_i$	*Rs*
0	13.7	13.7	0.0	0	11.8	11.8	0.0	0
30	7.0	2.6	4.4	1.1	11.1	9.9	1.3	1.0
40	6.3	1.6	4.7	1.4	10.9	9.2	1.8	1.3
50	5.4	0.5	4.9	1.7	10.8	8.6	2.2	1.6
70	4.2	−2.0	6.2	2.8	10.3	7.5	2.8	2.1
90	3.2	−3.4	6.6	3.0	9.9	6.5	3.4	2.3
110	2.2	−4.5	6.7	3.6	9.2	5.5	3.7	2.7

μ_i : 10^{-9} m^2 V^{-1} s^{-1}.

The interaction between the negatively charged HSA molecules and the positively charged basic chiral molecules was considered to be the main reason for efficient chiral discrimination of the tested basic compounds. The opposite charges of HSA and the analytes support the enantioseparation due to the optimal difference between the effective mobilities of the CS–enantiomer complexes and the free enantiomers [37,46]. The respective electrophoretic mobilities are listed in Table 1.

Association constants (K_A) were determined by analyzing the effective mobilities of enantiomers at various HSA concentrations. Binding curves for AML and VER are displayed in Figure 3A and B, respectively. K_A values of 22 620 M^{-1} for *R*-(+)-AML and 25 073 M^{-1} for *S*-(−)-AML were obtained when applying in the racemic mixture. This result showed the close agreement of enantiopure *S*-(−)-AML with K_A 25 101 M^{-1}. A clinical study by Luksa et al. has reported comparable pharmacokinetic parameters of the individual enantiomers after administration of racemic AML and enantiopure AML to healthy subjects. The close finding of *S*-(-)-AML K_A values in our study match up to the reported comparable pharmacokinetic parameters of AML in the racemic mixture and enantiopure [47]. Moreover, the K_A value of *S*-(−)-AML was obtained higher than *R*-(+)-AML, which was also found in a previous study by Liu et al. using FI-CE/FA [18].

Furthermore, *R*-(+)-VER (K_A 1844 M^{-1}) proved to bind stronger to HSA compared to *S*-(−)-VER (K_A 6.6 M^{-1}). However, a reliable binding curve could not be obtained for VER with HSA concentrations in the applied range of 30–110 μM. This is due to the weak interaction between VER enantiomers and HSA in the applied system, and binding curves are too straight to be evaluated quantitatively. Insufficient description of the binding curve leads to the unavoidable low accuracy of the binding constant prediction [37]. Indeed, the K_A values of VER enantiomers at certain CE conditions correspond to the relative measures of the complexes strength instead of apparent association constants. Despite the feasibility of the binding curves, the calculated K_A value of *R*-(+)-VER in the racemic mixture showed nearly the same value as that obtained in the earlier studies of racemic VER (K_A 1100–1790 M^{-1}) [19] and (K_A 1100 M^{-1}) [48].

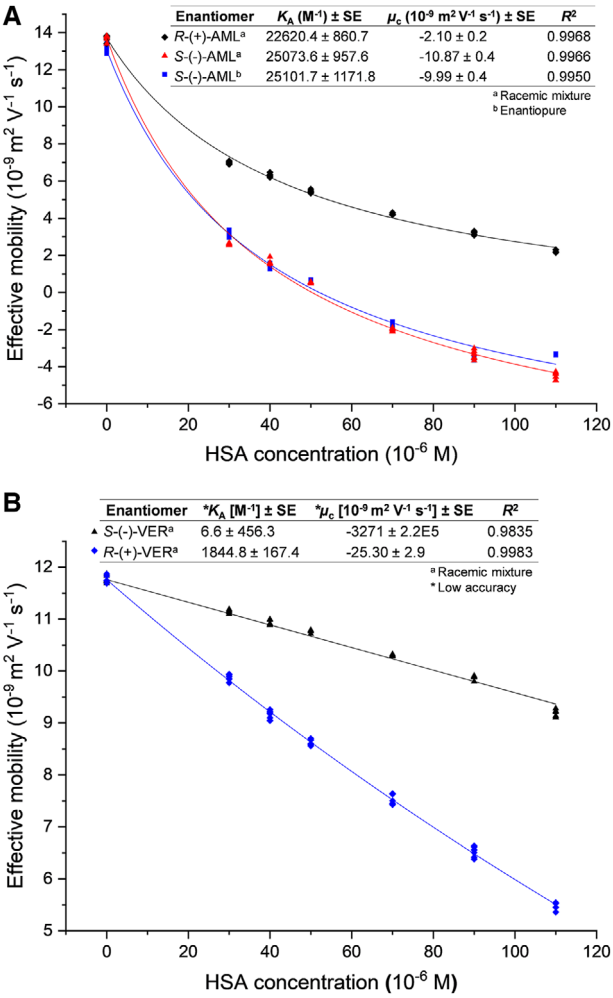

FIGURE 3 Binding curves of amlodipine (AML, 3A) and verapamil (VER, 3B) as a racemic mixture and pure enantiomer in the presence of 0–110 μM HSA

4 | CONCLUDING REMARKS

HSA chiral recognition ability has been successfully utilized in enantioselective interaction study toward selected basic drugs for enantiomeric separation and simultaneous binding constant determination by ms-ACE. The addition of HSA into the BGE solution at a physiological pH established an optimum difference in charges between the complexed form and the free drug, which resulted in different degrees of apparent mobilities. The nonlinear function of mobility shifts and HSA concentrations allows the determination of the binding affinity of the individual enantiomers, simultaneously. The binding constants of *R*-(+)-VER and *S*-(−)-AML were found to be higher than their antipodes when applying the racemic mixture. In addition, the K_A value of *S*-(−)-AML as pure enantiomer closely agrees with the K_A value of the *S*-(−)-enantiomer that measured in the racemic mixture. The binding affinity study proved that *S*-(−)-AML and *R*-(+)-VER bind stronger to human serum albumin compared to their counterparts.

Article Related Symbols

$\boldsymbol{\alpha}$, degree of the complexation; $\boldsymbol{a_1}$, a position of Gaussian component; $\boldsymbol{C_i}$, total concentration of the selector; $\boldsymbol{\Delta\mu_i}$, the effective mobility difference between two enantiomers; $\boldsymbol{K_A}$, association constant; **Rs**, resolution; $\boldsymbol{t_{1/2}}$, elimination half-life; $\boldsymbol{t_1}$, migration time of the first enantiomer; $\boldsymbol{t_2}$, migration time of the second enantiomer; $\mathbf{W}_{hh}$, peak width at half height; $\boldsymbol{\mu_c}$, fully saturated complex mobility; $\boldsymbol{\mu_f}$, free analyte mobility; $\boldsymbol{\mu_i}$, effective mobility, $\boldsymbol{\mu_{i_R}}$, effective mobility of *R*-(+)-enantiomer; $\boldsymbol{\mu_{i_S}}$, effective mobility of *S*-(−)-enantiomer.

ACKNOWLEDGMENTS

This study was supported by a research grant from Indonesia Endowment Fund for Education (LPDP), Ministry of Research, Technology and Higher Education (RISTEK DIKTI), Republic of Indonesia.

Open access funding enabled and organized by Projekt DEAL.

CONFLICT OF INTEREST

The authors have declared no conflict of interest.

ORCID

Ratih Ratih https://orcid.org/0000-0002-9308-2281
Sami El Deeb https://orcid.org/0000-0001-6417-4737

REFERENCES

1. Shen Z, Lv C, Zeng S. Significance and challenges of stereoselectivity assessing methods in drug metabolism. J Pharm Anal. 2016;6:1–10.
2. Levy RH, Boddy AV. Stereoselectivity in pharmacokinetics: A general theory. Pharm Res. 1991;8:551–6.
3. Li Z, Hage DS. Analysis of stereoselective drug interactions with serum proteins by high-performance affinity chromatography: A historical perspective. J Pharm Biomed Anal. 2017;144:12–24.
4. Chuang VTG, Otagiri M. Stereoselective binding of human serum albumin. Chirality 2006;18:159–66.
5. Hage DS. Analysis of biological interactions by affinity chromatography: Clinical and pharmaceutical applications. Clin Chem. 2017;63:1083–93.
6. Zhivkova ZD. Studies on drug–human serum albumin binding: The current state of the matter. Curr Pharm Des. 2015;21:1817–30.
7. Shen Q, Wang L, Zhou H, Jiang H-d, Yu L-s, Zeng S. Stereoselective binding of chiral drugs to plasma proteins. Acta Pharmacol Sin. 2013;34:998–1006.
8. Nayler WG. Amlodipine. Berlin: Springer-Verlag; 1993.
9. Knuuti J, Wijns W, Saraste A, Capodanno D, Barbato E, Funck-Brentano C, Prescott E, Storey RF, Deaton C, Cuisset T, Agewall S, Dickstein K, Edvardsen T, Escaned J, Gersh BJ, Svitil P, Gilard M, Hasdai D, Hatala R, Mahfoud F, Masip J, Muneretto C, Valgimigli M, Achenbach S, Bax JJ, ESC Scientific Document Group. 2019 ESC Guidelines for the diagnosis and management of chronic coronary syndromes: The Task Force for the diagnosis and management of chronic coronary syndromes of the European Society of Cardiology (ESC). Eur Heart J. 2020, 41:407–77.
10. Krasulova K, Holas O, Anzenbacher P. Influence of amlodipine enantiomers on human microsomal cytochromes P450: Stereoselective time-dependent inhibition of CYP3A enzyme activity. Molecules 2017;22:1–14.
11. Hancu G, Budău M, Kántor LK, Cârje A. Cyclodextrine screening for the chiral separation of amlodipine enantiomers by capillary electrophoresis. Adv Pharm Bull. 2015;5:35–40.
12. Perrotton T, Trompier D, Chang X-B, Di Pietro A, Baubichon-Cortay H. (R)- and (S)-verapamil differentially modulate the multidrug-resistant protein MRP1. J Biol Chem. 2007;282:31542–48.
13. Housaindokht MR, Zaeri ZR, Bahrololoom M, Chamani J, Bozorgmehr MR. Investigation of the behavior of HSA upon binding to amlodipine and propranolol: Spectroscopic and molecular modeling approaches. Spectrochim Acta A Mol Biomol Spectrosc. 2012;85:79–84.
14. Mallik R, Yoo MJ, Chen S, Hage DS. Studies of verapamil binding to human serum albumin by high-performance affinity chromatography. J Chromatogr B. 2008;876:69–75.
15. Yang J, Hage DS. Chiral Separations in capillary electrophoresis using human serum albumin as a buffer additive. Anal Chem. 1994;66:2719–25.
16. Zhu X, Ding Y, Lin B, Jakob A, Koppenhoefer B. Study of enantioselective interactions between chiral drugs and serum albumin by capillary electrophoresis. Electrophoresis 1999;20:1869–77.
17. Martínez-Gómez MA, Martínez-Pla JJ, Sagrado S, Villanueva-Camañas RM, Medina-Hernández MJ. Chiral separation of oxprenolol by affinity electrokinetic chromatography-partial filling technique using human serum albumin as chiral selector. J Pharm Biomed Anal. 2005;39:76–81.

18. Liu X, Song Y, Yue Y, Zhang J, Chen X. Study of interaction between drug enantiomers and human serum albumin by flow injection-capillary electrophoresis frontal analysis. Electrophoresis 2008;29:2876–83.
19. Ding YS, Zhu XF, Lin BC. Capillary electrophoresis study of human serum albumin binding to basic drugs. Chromatographia 1999;49:343–6.
20. Lu J, Ye F, Zhang A, Wei Z, Peng Y, Zhao S. Preparation and characterization of silica monolith modified with bovine serum albumin-gold nanoparticles conjugates and its use as chiral stationary phases for capillary electrochromatography. J Sep Sci. 2011;34:2329–36.
21. Qi L, Qiao J, Yang G, Chen Y. Chiral ligand-exchange CE assays for separation of amino acid enantiomers and determination of enzyme kinetic constant. Electrophoresis 2009;30: 2266–72.
22. Ding Y, Zhu X, Lin B. Study of interaction between drug enantiomers and serum albumin by capillary electrophoresis. Electrophoresis 1999;20:1890–4.
23. Ding Y, Zhu X, Lin B. Application of liquid pre-column capillary electrophoresis technique to the study of interaction between drug enantiomers and human serum albumin. Sci Chin. 1999;42:617–23.
24. Štěpánová S, Kašička V. Capillary electrophoretic methods applied to the investigation of peptide complexes. J Sep Sci. 2015;38:2708–21.
25. Jáč P, Scriba GKE. Recent advances in electrodriven enantioseparations. J Sep Sci. 2013;36:52–74.
26. Xu Y, Hong T, Chen X, Ji Y. Affinity capillary electrophoresis and fluorescence spectroscopy for studying enantioselective interactions between omeprazole enantiomer and human serum albumin. Electrophoresis 2017;38:1366–73.
27. Fanali S, Chankvetadze B. Some thoughts about enantioseparations in capillary electrophoresis. Electrophoresis 2019;40:2420–37.
28. Maddi S, Yamsani MR, Seeling A, Scriba GKE. Stereoselective plasma protein binding of amlodipine. Chirality 2010;22:262–6.
29. Asensi-Bernardi L, Martín-Biosca Y, Escuder-Gilabert L, Sagrado S, Medina-Hernández MJ. Evaluation of the enantioselective binding of imazalil to human serum albumin by capillary electrophoresis. Biomed Chromatogr. 2015;29:1637–42.
30. Haginaka J. In: Van Eeckhaut A, Michotte Y, eds. Chiral Separations by Capillary Electrophoresis: Chiral Separations using Proteins and Peptides as Chiral Selectors. New York: CRC Pres Taylor & Francis; 2010:139–62.
31. Nevídalová H, Michalcová L, Glatz Z. Capillary electrophoresis-based approaches for the study of affinity interactions combined with various sensitive and nontraditional detection techniques. Electrophoresis 2019, 40:625–42.
32. Wren SAC, Rowe RC, Payne RS. A theoretical approach to chiral capillary electrophoresis with some practical implications. Electrophoresis 1994;15:774–8.
33. Šolínová V, Mikysková H, Kaiser MM, Janeba Z, Holý A, Kašička V. Estimation of apparent binding constant of complexes of selected acyclic nucleoside phosphonates with β-cyclodextrin by affinity capillary electrophoresis. Electrophoresis 2016;37:239–47.
34. Riesová M, Svobodová J, Ušelová K, Tošner Z, Zusková I, Gaš B. Determination of thermodynamic values of acidic dissociation constants and complexation constants of profens and their utilization for optimization of separation conditions by Simul 5 complex. J Chromatogr A. 2014;1364:276–88.
35. Dubský P, Ördögová M, Malý M, Riesová M. CEval: All-in-one software for data processing and statistical evaluations in affinity capillary electrophoresis. J Chromatogr A. 2016;1445:158–65.
36. Krull IS, Gendreau CA, Dai HJ. In: Swartz ME, ed. Analytical Techniques in Combinatorial Chemistry: Capillary Electrophoresis in Combinatorial Library Analysis. New York: Marcel Dekker; 2000:137–72.
37. Stein M, Haselberg R, Mozafari-Torshizi M, Wätzig H. Experimental design and measurement uncertainty in ligand binding studies by affinity capillary electrophoresis. Electrophoresis 2019;40:1041–54.
38. Tanaka Y, Terabe S. Partial separation zone technique for the separation of enantiomers by affinity electrokinetic chromatography with proteins as chiral pseudo-stationary phases. J Chromatogr A. 1995;694:277–84.
39. Lelivère F, Gareil P. Selectivity in capillary electrophoresis: Application to chiral separations with cyclodextrins. Anal Chem. 1997;69:385–92.
40. Amini A, Westerlund D. Evaluation of association constants between drug enantiomers and human alpha 1-acid glycoprotein by applying a partial-filling technique in affinity capillary electrophoresis. Anal Chem. 1998;70:1425–30.
41. Olabi M, Stein M, Wätzig H. Affinity capillary electrophoresis for studying interactions in life sciences. Electrophoresis 2018;146:76–92.
42. Dixit S, Park JH. Application of rifampicin as a chiral selector for enantioresolution of basic drugs using capillary electrophoresis. J Chromatogr A. 2016;1453:138–42.
43. Hendrickx A, Mangelings D, Heyden Yv. In: Andrushko V, Andrushko N, eds. Stereoselective Synthesis of Drugs and Natural Products: Capillary Electrophoresis in Chiral Separations. Hoboken: John Wiley & Sons Inc.; 2013:1549–70.
44. Chankvetadze B. Contemporary theory of enantioseparations in capillary electrophoresis. J Chromatogr A. 2018;1567:2–25.
45. Chankvetadze B. Capillary Electrophoresis in Chiral Analysis. Chichester: John Wiley & Sons Ltd; 1997.
46. Chen Z, Weber SG. Determination of binding constants by affinity capillary electrophoresis, electrospray ionization mass spectrometry and phase-distribution methods. Trends Analyt Chem 2008, 27:738–48.
47. Lukša J, Josič Dj, Kremser M, Kopitar Z, Milutinovič S. Pharmacokinetic behaviour of R-(1)- and S-(2)-amlodipine after single enantiomer administration. J Chromatogr B. 1997;703:185–93.
48. Jia Z, Ramstad T, Zhong M. Determination of protein-drug binding constants by pressure-assisted capillary electrophoresis (PACE)/frontal analysis (FA). J Pharm Biomed Anal. 2002;405–13.

How to cite this article: Ratih R, Wätzig H, Stein M, El Deeb S. Investigation of the enantioselective interaction between selected drug enantiomers and human serum albumin by mobility shift-affinity capillary electrophoresis. *J Sep Sci*. 2020;43:3960–3968.
https://doi.org/10.1002/jssc.202000372

ISSN 1615-9306 · JSSCCJ 43 (20) 3825–3982 (2020) · Vol. 43 · No. 20 · October 2020 · D 10609

JSS

JOURNAL OF SEPARATION SCIENCE

20|20

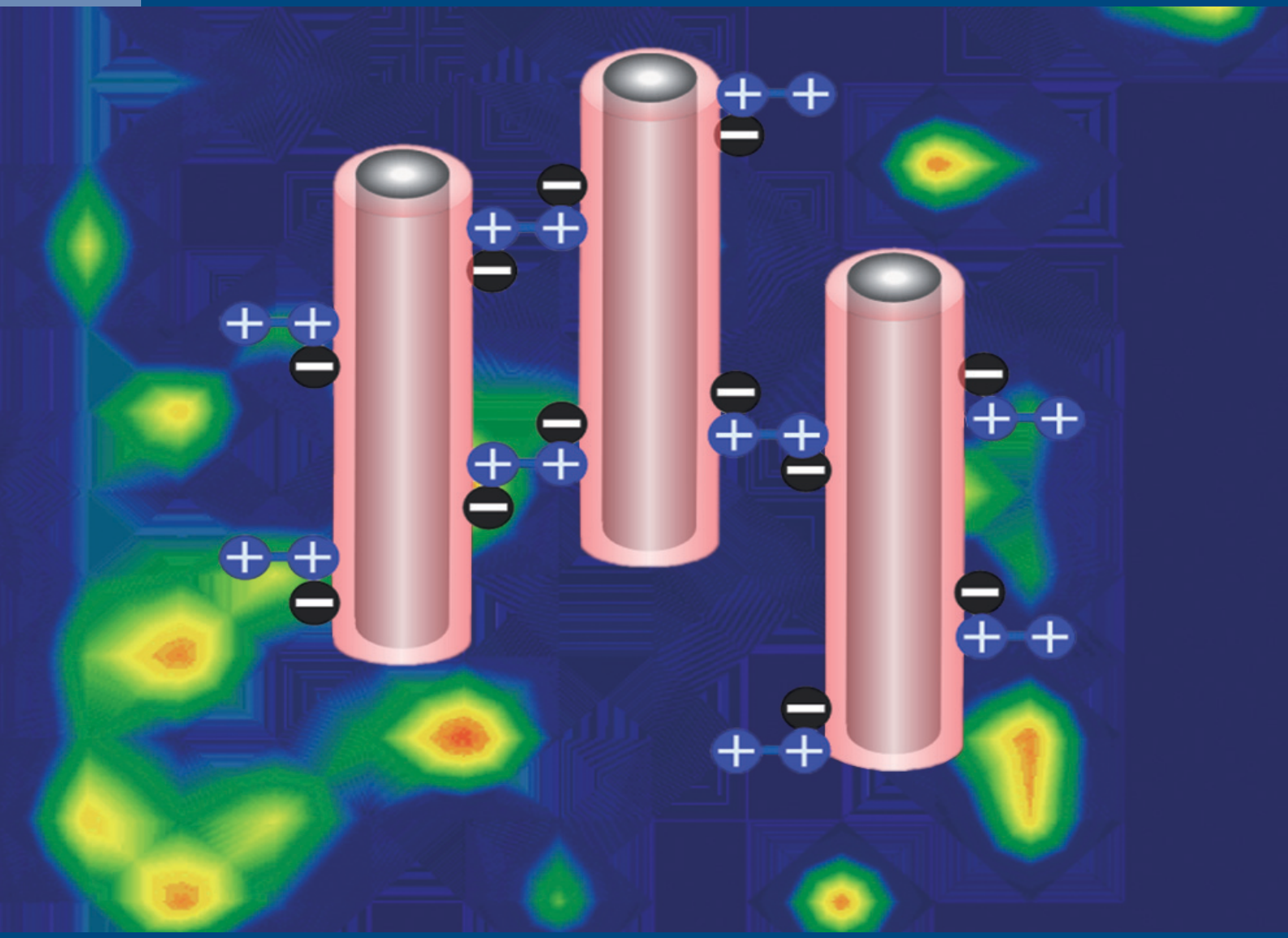

Methods
Chromatography · Electroseparation

Applications
Biomedicine · Foods · Environment

www.jss-journal.com

WILEY-VCH

Journal of Separation Science

Journal Management

Eva-Stina Mueller
esmueller@wiley.com

Marketing

Sonja Kwiatkowskyj
skwiatkows@wiley.com

Production, Reprints

Birgit Hill
bhill@wiley.com

Copyright Permissions

rights@wiley-vch.de

Web Editor

Lukas Quinn
lquinn@wiley.com

Office Manager

Jennifer Rodden (UK)
jss@wiley-vch.de

Notice to Authors

Please refer to the journal's home page
www.jss-journal.com

Publisher

Wiley-VCH GmbH
P.O. Box 10 11 61
D-69451 Weinheim (Germany)
Tel.: +49-6201-606-0
Fax: +49-6201-606-207
jss@wiley-vch.de

CASSS
AN INTERNATIONAL SEPARATION SCIENCE SOCIETY

EuSSS

Back

JOURNAL OF SEPARATION SCIENCE

Volume 43, Issue 20

Pages: 3826-3982
October 2020

< Previous Issue | Next Issue >

GO TO SECTION

Export Citation(s)

FRONT COVER

Free Access

Front Cover

First Published: 22 October 2020

PDF | Request permissions

EDITORIAL BOARD

Free Access

Issue Information

Pages: 3826 | First Published: 22 October 2020

Back

CONTENTS

LIQUID CHROMATOGRAPHY

Back

Enantioselective residue analysis of oxathiapiprolin and its metabolite in tea and other crops by ultra-high performance liquid chromatography–tandem mass spectrometry

Xinzhong Zhang, Hezhi Sun, Xinru Wang, Hongxia Li, Qing Zhong, Fengjian Luo, Zongmao Chen

Pages: 3856-3867 | First Published: 10 August 2020

Abstract | Full text | PDF | References | Request permissions

Simultaneous separation and indirect ultraviolet detection of chlorate and perchlorate by pyridinium ionic liquids in reversed-phase liquid chromatography

Zhen-jie Yin, Ya-nan Zhang, Fu-jing Guan, Hong Yu, Ya-jie Ma

Pages: 3868-3875 | First Published: 10 August 2020

Abstract | Full text | PDF | References | Request permissions

Development of an ultra-high-performance liquid chromatography-charged aerosol detection/UV method for the quantitation of linear polyethylenimines in oligonucleotide polyplexes

Adam Socia, Yong Liu, Yuejie Zhao, Andreas Abend, W. Peter Wuelfing

Pages: 3876-3884 | First Published: 12 August 2020

Abstract | Full text | PDF | References | Request permissions

HPLC coupled with electrospray ionization multistage MS/MS and TLC analysis of flavones-C-glycosides and bibenzyl of *Dendrobium hercoglossum*

Li Hu, Chujuan Zhou, Yue-Chun Huang, Yawen Wang, Gang Wei, Zhiyun Liang, Chunhua Zhou

Pages: 3885-3901 | First Published: 16 August 2020

Abstract | Full text | PDF | References | Request permissions

A simple, cost-effective, and rapid separation process for the isolation of anticoagulant active fraction from the fruit extract of *Momordica charantia*: Characterization of bioactive components and anticoagulant mechanism of active fraction in a mouse model

Debananda Gogoi, Shambhavi Jha, Pronobesh Chattopadhyay, Ashis K. Mukherjee

Pages: 3902-3912 | First Published: 24 August 2020

Abstract | Full text | PDF | References | Request permissions

Back

spectrometry for large-scale identification of proteins interact with immunoglobulin G in HeLa cells

Feng Qin, Xuantang Wang, Guoquan Yan, Mingxia Gao, Xiangmin Zhang

Pages: 3913-3920 | First Published: 24 August 2020

Abstract | Full text | PDF | References | Request permissions

Simultaneous determination of acetamiprid and 6-chloronicotinic acid in environmental samples by using ion chromatography hyphenated to online photoinduced fluorescence detector

Qamar Subhani, Nadeem Muhammad, Zhouman Huang, Muhammad Asif, Irshad Hussain, Muhammad Zahid, Cui Hairong, Yan Zhu, Dandan Guo

Pages: 3921-3930 | First Published: 25 August 2020

Abstract | Full text | PDF | References | Request permissions

SAMPLE PREPARATION

Evaluation and optimization of the derivatization reaction conditions of glyphosate and aminomethylphosphonic acid with 6-aminoquinolyl-N-hydroxysuccinimidyl carbamate using reversed-phase liquid chromatography

Clàudia Fontàs, Juan M. Sanchez

Pages: 3931-3939 | First Published: 12 August 2020

Abstract | Full text | PDF | References | Request permissions

Determination of trace polycyclic aromatic hydrocarbons in water and milk using solid-phase extraction packed with graphene/chitosan composite aerogel prior to gas chromatography–mass spectrometry

Yuanji Gao, Yunan Qin, Feng Xiong, Lijuan Zhao

Pages: 3940-3948 | First Published: 15 August 2020

Back

ELECTRODRIVEN SEPARATION

Capillary electrophoretic profiling of in-bone tryptic digests of proteins as a potential tool for the detection of inflammatory states in oral surgery

Iva Michalusová, Petra Sázelová, Pavel Cejnar, Štěpánka Kučková, Radovan Hynek, Václav Kašička

Pages: 3949-3959 | First Published: 11 August 2020

Abstract | Full text | PDF | References | Request permissions

Open Access

Investigation of the enantioselective interaction between selected drug enantiomers and human serum albumin by mobility shift-affinity capillary electrophoresis

Ratih Ratih, Hermann Wätzig, Matthias Stein, Sami El Deeb

Pages: 3960-3968 | First Published: 21 August 2020

Abstract | Full text | PDF | References | Request permissions

OTHER TECHNIQUES

Electrochemical microreactor combined with mass spectrometry for online oxidation and real-time detection of alkaloids

Juan Yang, Li-Hong Ye, Bin Wang, Hui Zheng, Jun Cao

Pages: 3969-3981 | First Published: 21 August 2020

Abstract | Full text | PDF | References | Request permissions

Back

Free Access

Corrigendum

Pages: 3982 | First Published: 22 October 2020

This article corrects the following:

Open-tubular capillary electrochromatographic application of a sol-gel matrix with chilli peppers, garlic, or synthetic additives

Jana Svobodová,Ivan Mikšík

Volume 43, Issue 18, Journal of Separation Science | pages: 3691-3701 |
First Published online: July 30, 2020

Full text | PDF | Request permissions

An Organ of the European Society for Separation Science

More from this journal

Special Issue Dedicated to our Editor in Chief, Frantisek Svec, on the Occasion of his 75th Birthday (Virtu Special Issue)
Molecular Imprinting in Separation Science (Virtual Special Issue)

Back

Biomarkers, Proteins, Peptides (Virtual Special Issue)

Sample Preparation in Mass Spectrometry (Virtual Special Issue)

Journal of Separation Science

COUNTRY	SUBJECT AREA AND CATEGORY	PUBLISHER	H-INDEX
Germany	Chemical Engineering Filtration and Separation Chemistry Analytical Chemistry	Wiley-VCH Verlag	110

PUBLICATION TYPE	ISSN	COVERAGE	INFORMATION

Journals 16159314, 16159306 2000-2022

Homepage

How to publish in this journal

svecfr@faf.cuni.cz

SCOPE

The Journal of Separation Science (JSS) is the most comprehensive source in separation science, since it covers all areas of chromatographic and electrophoretic separation methods in theory and practice, both in the analytical and in the preparative mode, solid phase extraction, sample preparation, and related techniques. Manuscripts on methodological or instrumental developments, including detection aspects, in particular mass spectrometry, as well as on innovative applications will also be published. Manuscripts on hyphenation, automation, and miniaturization are particularly welcome. Pre- and post-separation facets of a total analysis may be covered as well as the underlying logic of the development or application of a method.

Quartiles

FIND SIMILAR JOURNALS

1	2	3	4
Chromatographia	**Journal of Chromatography A**	**Separations**	**Journal of Li Chromatogr**
DEU	NLD	CHE	USA
88% similarity	**80%** similarity	**75%** similarity	**7** si

SJR

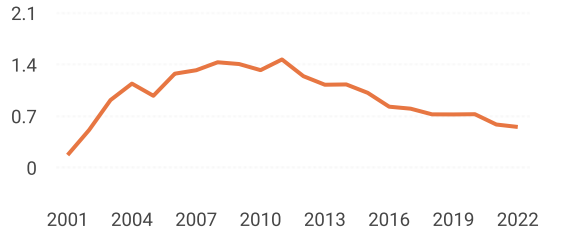

Total Documents

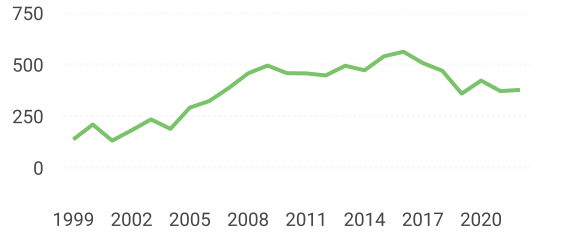

Total Cites Self-Cites

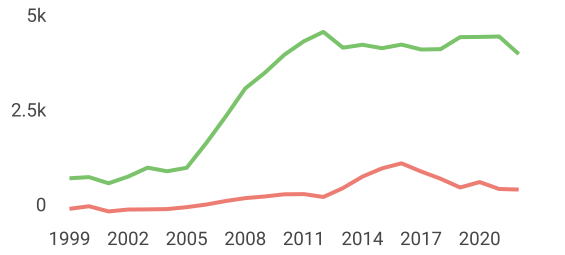

Citations per document

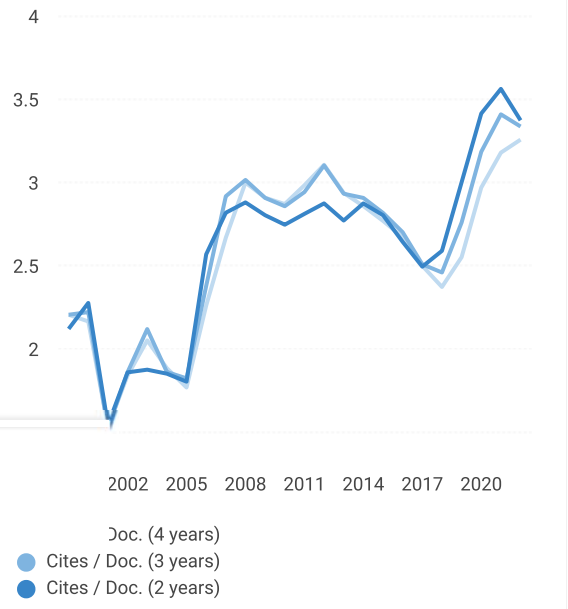

External Cites per Doc Cites per Doc

% International Collaboration

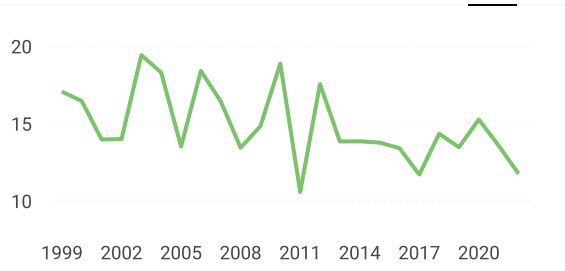

Citable documents Non-citable documents

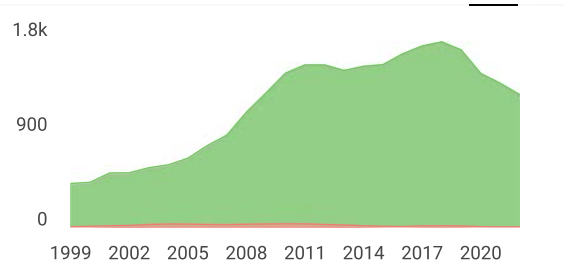

Cited documents Uncited documents

Show this widget in your own website

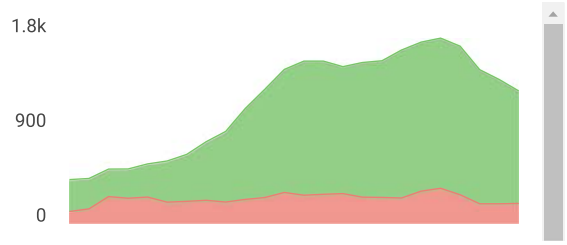

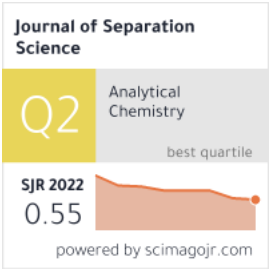

← Just copy the code below and paste within your html code:

<a href="https://www.scimag

SCImago Graphica

Explore, visually communicate and make sense of data with our **new data visualization tool**.

Metrics based on Scopus® data as of April 2023

Leave a comment

Name

Email
(will not be published)

I'm not a robot
reCAPTCHA
Privacy - Terms

Submit

The users of Scimago Journal & Country Rank have the possibility to dialogue through comments linked to a specific journal. The purpose is to have a forum in which general doubts about the processes of publication in the journal, experiences and other issues derived from the publication of papers are resolved. For topics on particular articles, maintain the dialogue through the usual channels with your editor.

Developed by: SCImago

Powered by: Scopus

Follow us on @ScimagoJR

EST MODUS IN REBUS
Horatio (Satire 1,1,106)

Cookie settings

Cookie policy

Source details

Journal of Separation Science

Incorporating: Journal of Microcolumn Separations

Formerly known as: HRC Journal of High Resolution Chromatography

Scopus coverage years: from 2000 to Present

Publisher: Wiley-Blackwell

ISSN: 1615-9306 E-ISSN: 1615-9314

Subject area: Chemistry: Analytical Chemistry | Chemical Engineering: Filtration and Separation

Source type: Journal

CiteScore 2022
6.0

SJR 2022
0.547

SNIP 2022
0.869

View all documents > | Set document alert | Save to source list | Source Homepage

CiteScore | CiteScore rank & trend | Scopus content coverage

CiteScore 2022

$$6.0 = \frac{9{,}052 \text{ Citations } 2019 - 2022}{1{,}511 \text{ Documents } 2019 - 2022}$$

Calculated on 05 May, 2023

CiteScoreTracker 2023

$$6.0 = \frac{8{,}024 \text{ Citations to date}}{1{,}346 \text{ Documents to date}}$$

Last updated on 05 September, 2023 • Updated monthly

CiteScore rank 2022

Category	Rank	Percentile
Chemistry Analytical Chemistry	#41/141	71st
Chemical Engineering Filtration and Separation	#7/20	67th

View CiteScore methodology > | CiteScore FAQ > | Add CiteScore to your site

About Scopus

What is Scopus

Content coverage

Scopus blog

Scopus API

Privacy matters

Language

日本語版を表示する

查看简体中文版本

查看繁體中文版本

Просмотр версии на русском языке

Customer Service

Help

Tutorials

Contact us